14

Axisymmetric Solid Benchmark Problems

TABLE OF CONTENTS

This chapter presents three benchmark examples that are often used to assess the performance of FEM models for axisymmetric solid analysis.

They were previously included as part of Chapter 13, but have been split to a new Chapter on account of length.

§14.1. Benchmark 1: Internally Pressurized Thick Cylinder

The first benchmark problem is that used in the previous Chapter to illustrate driver script preparation for the `QuadSOR` code. It is illustrated in Figure 14.1, which reproduces Figure 13.1 for convenience. The study in the present Section covers: effect of mesh refinement in the radial direction, relative performance of 4-node versus 8-node quadrilateral elements, and influence of Poisson ratio ν when passing from $\nu = 0$ to near the incompressible limit $\nu \approx \frac{1}{2}$.

§14.1.1. Problem Description

Restating the problem: a cylindrical hollow tube of inner radius a and outer radius b is subjected to internal pressure p. The tube and its cross section are shown in Figure 14.1. The tube extends indefinitely along the z axis and is in a plane strain state along that direction. The material is isotropic with elastic modulus E and Poisson's ratio ν. A "slice" of thickness d is extracted and discretized as shown in Figure 14.2 using using N_{er} quadrilateral ring elements along the radial direction r and one along the axial direction z (In that Figure, N_{er} are 4 and 2 for the 4-node and 8-node quadrilateral meshes, respectively.) Nodes move in the radial direction only, which results in the support conditions drawn in Figure 14.2(b,c).

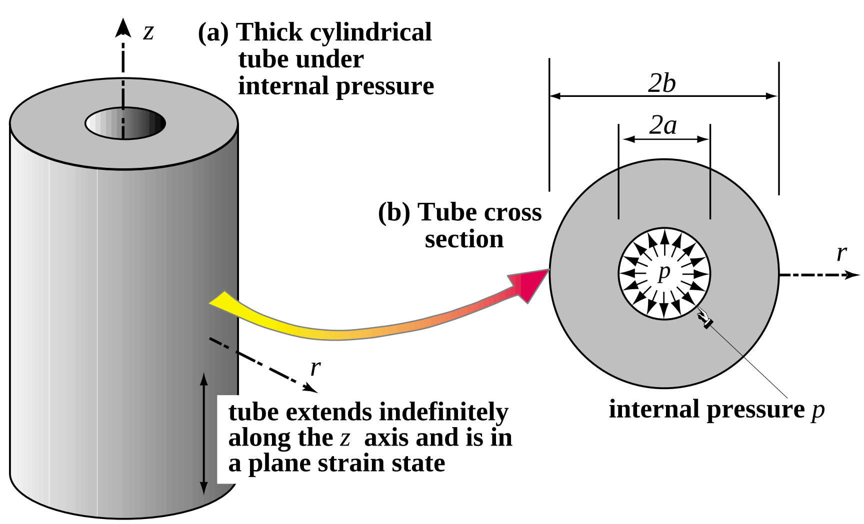

FIGURE 14.1. Pressurized thick cylinder benchmark problem. Reproduced from Figure 13.1 for convenience.

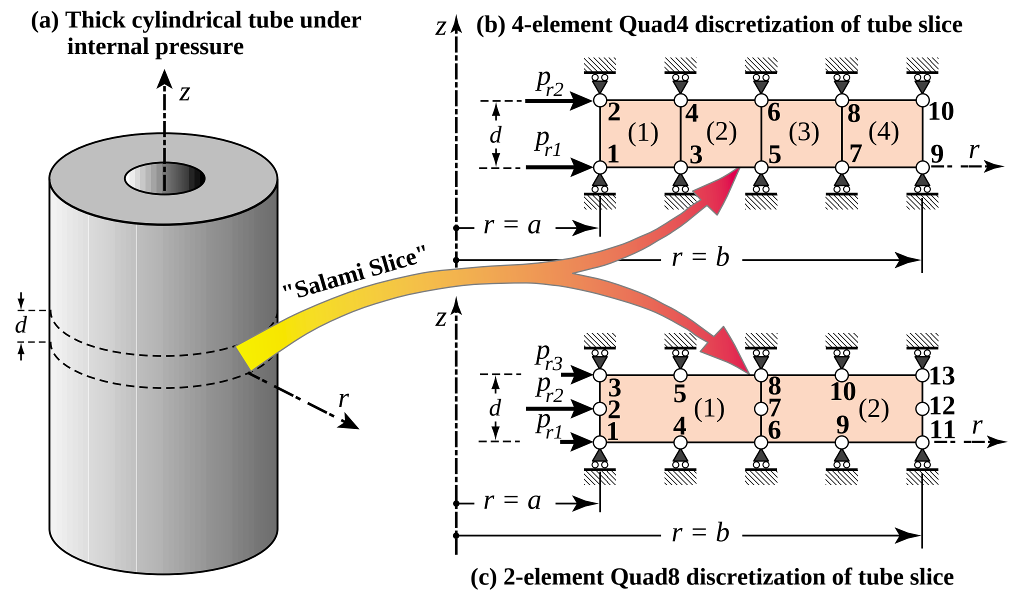

FIGURE 14.2. Two example FEM discretizations for the pressurized thick cylinder benchmark.

§14.1.2. Exact Solution

The exact stress distribution[1] across the wall is

$$\sigma_{rr} = p\frac{a^2}{b^2-a^2}\left(1-\frac{b^2}{r^2}\right), \qquad \sigma_{zz} = p\frac{2a^2\nu}{b^2-a^2},$$
$$\sigma_{\theta\theta} = p\frac{a^2}{b^2-a^2}\left(1+\frac{b^2}{r^2}\right), \qquad \text{others zero.} \tag{14.1}$$

Note that $\sigma_{zz}=0$ if $\nu=0$ and that $\sigma_{rr}+\sigma_{\theta\theta}$ does not depend on r. Transforming this stress field to strains through $\mathbf{e}=\mathbf{E}^{-1}\boldsymbol{\sigma}$ gives the exact strain field, which can be verified to satisfy $e_{zz}=0$. The hoop strain thus obtained is $e_{\theta\theta}=pa^2\,(1+\nu)\,(b^2+r^2(1-2\nu))/(E(b^2-a^2)r^2)$, which multiplied by r yields the exact radial displacement

$$u_r = p\frac{a^2(1+\nu)(b^2+r^2(1-2\nu))}{E(b^2-a^2)r}. \tag{14.2}$$

§14.1.3. Driver Script

The *Mathematica* driver script listed in Figure 14.3 accepts both 4-node and 8-node quad elements. Note that geometric, constitutive and discretization properties are declared at the top to make parametrization simpler. To set the element type it is sufficient to declare `etype` in the second line of the script to be either `"Quad4"` or `"Quad8"`. The number of elements along the radial and axial directions: N_{er} and N_{ez}, are parametrized by the values assigned to `Ner` and `Nez`, respectively. The latter is assumed to be 1 since the solution only depends on r.

[1] Taken from S. Timoshenko and J. N. Goodier, *Theory of Elasticity*, McGraw-Hill, 2nd ed., 1951, Chapter 4, for a condition of plane strain in the z direction. The solution is due to G. Lamé, *Leçons sur la Théorie Mathématique de l'Elasticité des Corps Solides*, Paris, Bachellier, 1852.

```
ClearAll[Em,ν,th,a,b,d,p,Ner,Nez];
Em=1000.; ν=0.0; etype="Quad4"; numer=True; Ner=4; Nez=1;
Kfac=1; a=4; b=10; d=2; aspect=d/(b-a); p=10;

(*  Define FEM model *)

MeshCorners=N[{{a,0},{b,0},{b,d},{a,d}}];
If [etype=="Quad4",
    NodeCoordinates=GenQuad4NodeCoordinates[MeshCorners,Ner,Nez];
    ElemNodes=GenQuad4ElemNodes[Ner,Nez]];
If [etype=="Quad8",
    NodeCoordinates=GenQuad8NodeCoordinates[MeshCorners,Ner,Nez];
    ElemNodes=GenQuad8ElemNodes[Ner,Nez]];
numnod=Length[NodeCoordinates]; numele=Length[ElemNodes];
ElemType=Table[etype,{numele}];
ElemMaterial=Table[N[{Em,ν}],{numele}];
FreedomTags=Table[{0,1},{numnod}];
FreedomValues=Table[{0,0},{numnod}]; pfor=N[Kfac*p*a*d];
If [etype=="Quad4",
    FreedomValues[[1]]=FreedomValues[[2]]={pfor/2,0}];
If [etype=="Quad8",
    FreedomValues[[1]]=FreedomValues[[3]]={pfor/6,0};
    FreedomValues[[2]] ={2*pfor/3,0}];
ElemBodyForces= ElemTractionForces={}; DefaultOptions={numer};
(* Problem data print statements removed *)
Plot2DElementsAndNodes[NodeCoordinates,ElemNodes,aspect,
      "Press thick cylinder",True,True];

(*  Solve problem and print results *)

{NodeDisplacements,NodeForces,NodeStresses}=RingAnalysisDriver[
    NodeCoordinates,ElemType,ElemNodes,
    ElemMaterial,ElemBodyForces,ElemTractionForces,
    FreedomTags,FreedomValues,DefaultOptions];
PrintRingAnalysisSolution[NodeDisplacements,NodeForces,
     NodeStresses,"Computed solution",{}];
{ExactNodeDisplacements,ExactNodeStresses}=
     ExactSolution[NodeCoordinates,{a,b},{Em,ν,ρ},p,
     "PressThickCylinder",numer];
PrintRingNodeDispStresses[ExactNodeDisplacements,
    ExactNodeStresses,"Exact (Lame) solution",{}];

(* Contour plots of stress distributions *)

legend={(a+b)/2,0.75*d}; whichones={True,True,True,False};
If [ν==0, whichones={True,False,True,False}];
ContourPlotStresses[NodeCoordinates,ElemNodes,NodeStresses,
  whichones,True,{},legend,aspect];

(* Radial plots comparing FEM vs exact solutions *)

pwhat={"ur","σrr","σzz","σθθ"};
For [ip=1,ip<=Length[pwhat],ip++, what=pwhat[[ip]];
     RadialPlotFEMvsExact[etype,NodeCoordinates,NodeDisplacements,
       NodeStresses,{a,b},{Em,ν,ρ},p,{Ner,Nez},
      "PressThickCylinder",what,1,numer]  ];
```

FIGURE 14.3. Driver script for pressurized thick cylinder benchmark. This one accepts both Quad4 and Quad8 elements, as well as (through mesh generation) arbitrary number of elements in the radial direction.

If the element type is "Quad4" a regular mesh is generated by modules GenQuad4NodeCoordinates and GenQuad4ElemNodes, described in the previous Chapter. If the element type is Quad8 the generation modules invoked are GenQuad8NodeCoordinates and GenQuad8ElemNodes. the element type is "Quad8". Pressure lumping to the nodes on the inner radius $r = a$ depends on element type. The total pressure force is $p_{for} = K_{fac}\, p\, a\, d$, in which $K_{fac} = 1$ for QuadSOR because it uses a one-radian circumferential ring span. That value is stored in pfor. If the element type is "Quad4", the two innermost nodes 1 and 2 receive $\frac{1}{2}\, p_{for}$ each. If the element type is "Quad8" the three innermost nodes 1, 2 and 3 receive $\frac{1}{6}\, p_{for}$, $\frac{2}{3}\, p_{for}$ and $\frac{1}{6}\, p_{for}$, respectively, in accordance with consistent node force lumping.

§14.1.4. Results For Zero Poisson Ratio

The results presented here were computed for $a = 4$, $b = 10$, $d = 2$, $p = 10$, $E = 1000$, two Poisson ratio values, two element types, and two radial discretizations for each type.

The script of Figure 14.3 specifically sets etype="Quad4", Ner=4 and $\nu = 0$. The mesh is actually that pictured in Figure 14.2(b). Computed and exact nodal values are tabulated in Figure 14.4. Radial displacements u_r, radial stresses σ_{rr} and hoop stresses $\sigma_{\theta\theta}$ are graphically compared over the wall $a \leq r \leq b$ with the exact solution in Figure 14.5(a).

As can be seen u_r and $\sigma_{\theta\theta}$ are satisfactorily predicted. The hole-edge radial stress, however, is significantly underestimated: $\sigma_{rr} = -6.604$ compared to the exact $\sigma_{rr} = -p = -10$. This is a consequence of the impossibility of doing interelement stress averaging at that high-stress-gradient edge. For this low-order model the variation of σ_{rr} in the r direction is limited to be constant within the element. Thus $\sigma_{rr} = -6.604$ is more representative of the stress at the center of element (1). The σ_{rr} agreement at other nodes is reasonable given the coarseness of the mesh. The higher accuracy of the hoop stress $\sigma_{\theta\theta}$ is incidental, reflecting an idiosyncracy of axisymmetric solids: the hoop strain $\epsilon_{\theta\theta} = u_r/r$ is not obtained through displacement differentiation. It thus attains the same accuracy as u_r. And for zero ν, $\sigma_{\theta\theta} = E\,\epsilon_{\theta\theta} = E\,u_r/r$.

Increasing Ner to 16 gives a solution that is compared with the exact one in Figure 14.5(b). Both u_r and $\sigma_{\theta\theta}$ are correct to at least 3 places. The only visible flaw is the discrepancy of σ_{rr} at the hole boundary, where it gives $\sigma_{rr} = -8.965$ instead of $-p = -10$. Again this is a consequence of lack of interelement averaging. Away from the hole σ_{rr} agrees with the exact solution to plot accuracy.

The analysis is then redone with the 8-node quadrilateral Quad8 with reduced (2×2) integration. To make a fair comparison with Quad4, the Quad8 meshes contain half the elements: 2 and 8, respectively, which results in a similar number of nodes.

The results of running Quad8 with Ner=2 are tabulated in Figure 14.6. Radial displacements u_r, radial stresses σ_{rr} and hoop stresses $\sigma_{\theta\theta}$ are graphically compared over $a \leq r \leq b$ with the exact solution in Figure 14.7(a). This element is supposed to be nodally exact for one-dimensional problems, and indeed the computed and exact u_r may be verified to agree numerically to 15 places at all nodes. The hoop stress should be also nodally exact since $\sigma_{\theta\theta} = E\,u_r/r$, but the extrapolation from Gauss points introduces discrepancies. The computed radial stress σ_{rr} is as good as can be expected from a linear variation over the element.

Running Quad8 with Ner=8 give the results plotted in Figure 14.7(b). Again the displacements are nodally exact. Both σ_{rr} and $\sigma_{\theta\theta}$ agree everywhere with the exact solution at plot accuracy.

Computed solution

node	r-disp	z-disp	sigma-rr	sigma-zz	sigma-θθ	sigma-rz	r-force	z-force
1	0.0546	0.0000	−6.6040	0.0000	13.3193	0.0000	40.0000	0.0000
2	0.0546	0.0000	−6.6040	0.0000	13.3193	0.0000	40.0000	0.0000
3	0.0447	0.0000	−4.7954	0.0000	7.9555	0.0000	0.0000	0.0000
4	0.0447	0.0000	−4.7954	0.0000	7.9555	0.0000	0.0000	0.0000
5	0.0402	0.0000	−2.1293	0.0000	5.6858	0.0000	0.0000	0.0000
6	0.0402	0.0000	−2.1293	0.0000	5.6858	0.0000	0.0000	0.0000
7	0.0383	0.0000	−0.7984	0.0000	4.4821	0.0000	0.0000	0.0000
8	0.0383	0.0000	−0.7984	0.0000	4.4821	0.0000	0.0000	0.0000
9	0.0379	0.0000	−0.3250	0.0000	3.7674	0.0000	0.0000	0.0000
10	0.0379	0.0000	−0.3250	0.0000	3.7674	0.0000	0.0000	0.0000

Exact (Lame) solution

node	r-disp	z-disp	sigma-rr	sigma-zz	sigma-θθ	sigma-rz
1	0.0552	0.0000	−10.0000	0.0000	13.8095	0.0000
2	0.0552	0.0000	−10.0000	0.0000	13.8095	0.0000
3	0.0451	0.0000	−4.3920	0.0000	8.2015	0.0000
4	0.0451	0.0000	−4.3920	0.0000	8.2015	0.0000
5	0.0405	0.0000	−1.9825	0.0000	5.7920	0.0000
6	0.0405	0.0000	−1.9825	0.0000	5.7920	0.0000
7	0.0386	0.0000	−0.7316	0.0000	4.5411	0.0000
8	0.0386	0.0000	−0.7316	0.0000	4.5411	0.0000
9	0.0381	0.0000	0.0000	0.0000	3.8095	0.0000
10	0.0381	0.0000	0.0000	0.0000	3.8095	0.0000

FIGURE 14.4. Pressurized thick cylinder benchmark: computed and exact nodal solution for 4-element Quad4 model with Poisson ratio $\nu = 0$. The mesh is that shown in Figure 14.2(b).

(a) 4 x 1 Mesh of Quad4 Elements, ν = 0:

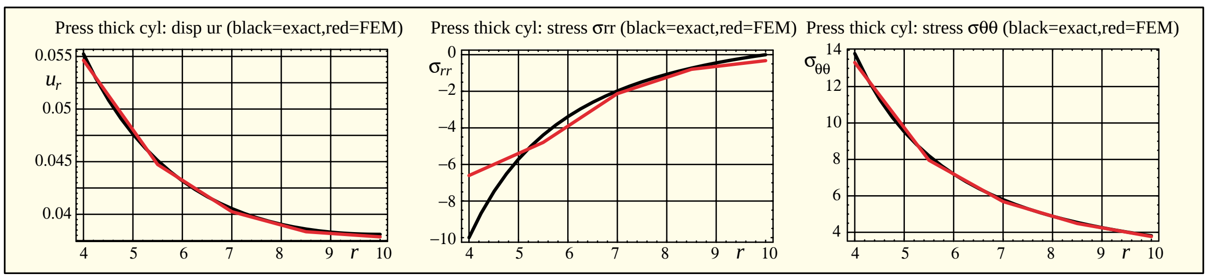

(b) 16 x 1 Mesh of Quad4 Elements, ν = 0:

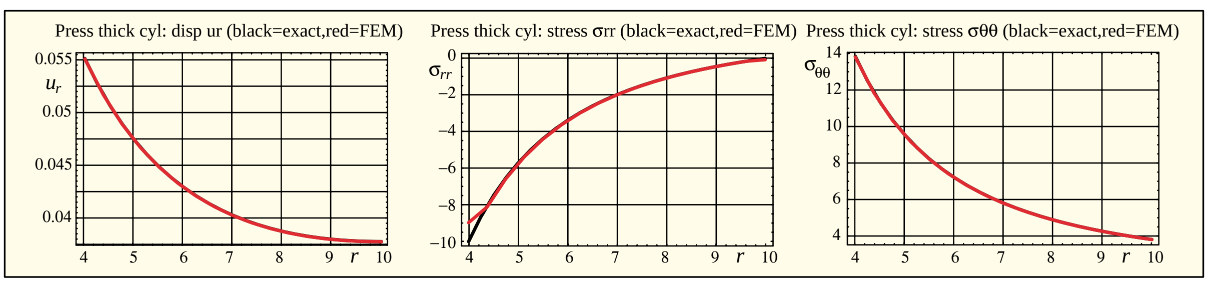

FIGURE 14.5. Pressurized thick cylinder benchmark: r plots of computed versus exact u_r, σ_{rr} and $\sigma_{\theta\theta}$ for Quad4 meshes with $\nu = 0$: (a) 4-element mesh, (b) 16-element mesh.

§14.1.5. Results For Near Incompressible Material

If Poisson ratio is increased over zero, `Quad4` results gradually lose accuracy if the number of elements is kept the same. In the limit $\nu \to \frac{1}{2}$, the material approaches incompressibility, and the computed solution deterioration accelerates. This phenomenon is known as *volumetric locking* in the FEM literature. To illustrate that degradation, the 4-element `Quad4` mesh is run with $\nu = 0.499$,

Computed solution

node	r–disp	z–disp	sigma–rr	sigma–zz	sigma–θθ	sigma–rz	r–force	z–force
1	0.0552	0.0000	−8.6085	0.0000	12.4181	0.0000	13.3333	0.0000
2	0.0552	0.0000	−8.6085	0.0000	12.4181	0.0000	53.3333	0.0000
3	0.0552	0.0000	−8.6085	0.0000	12.4181	0.0000	13.3333	0.0000
4	0.0451	0.0000	−4.8980	0.0000	8.7075	0.0000	0.0000	0.0000
5	0.0451	0.0000	−4.8980	0.0000	8.7075	0.0000	0.0000	0.0000
6	0.0405	0.0000	−1.4820	0.0000	5.2916	0.0000	0.0000	0.0000
7	0.0405	0.0000	−1.4820	0.0000	5.2916	0.0000	0.0000	0.0000
8	0.0405	0.0000	−1.4820	0.0000	5.2916	0.0000	0.0000	0.0000
9	0.0386	0.0000	−0.8163	0.0000	4.6259	0.0000	0.0000	0.0000
10	0.0386	0.0000	−0.8163	0.0000	4.6259	0.0000	0.0000	0.0000
11	0.0381	0.0000	0.1441	0.0000	3.6655	0.0000	0.0000	0.0000
12	0.0381	0.0000	0.1441	0.0000	3.6655	0.0000	0.0000	0.0000
13	0.0381	0.0000	0.1441	0.0000	3.6655	0.0000	0.0000	0.0000

Exact (Lame) solution

node	r–disp	z–disp	sigma–rr	sigma–zz	sigma–θθ	sigma–rz
1	0.0552	0.0000	−10.0000	0.0000	13.8095	0.0000
2	0.0552	0.0000	−10.0000	0.0000	13.8095	0.0000
3	0.0552	0.0000	−10.0000	0.0000	13.8095	0.0000
4	0.0451	0.0000	−4.3920	0.0000	8.2015	0.0000
5	0.0451	0.0000	−4.3920	0.0000	8.2015	0.0000
6	0.0405	0.0000	−1.9825	0.0000	5.7920	0.0000
7	0.0405	0.0000	−1.9825	0.0000	5.7920	0.0000
8	0.0405	0.0000	−1.9825	0.0000	5.7920	0.0000
9	0.0386	0.0000	−0.7316	0.0000	4.5411	0.0000
10	0.0386	0.0000	−0.7316	0.0000	4.5411	0.0000
11	0.0381	0.0000	0.0000	0.0000	3.8095	0.0000
12	0.0381	0.0000	0.0000	0.0000	3.8095	0.0000
13	0.0381	0.0000	0.0000	0.0000	3.8095	0.0000

FIGURE 14.6. Pressurized thick cylinder benchmark: computed and exact nodal solution for 2-element Quad8 model with Poisson ratio $\nu = 0$. The mesh is that shown in Figure 14.2(c).

(a) 2 x 1 Mesh of Quad8 Elements, ν = 0:

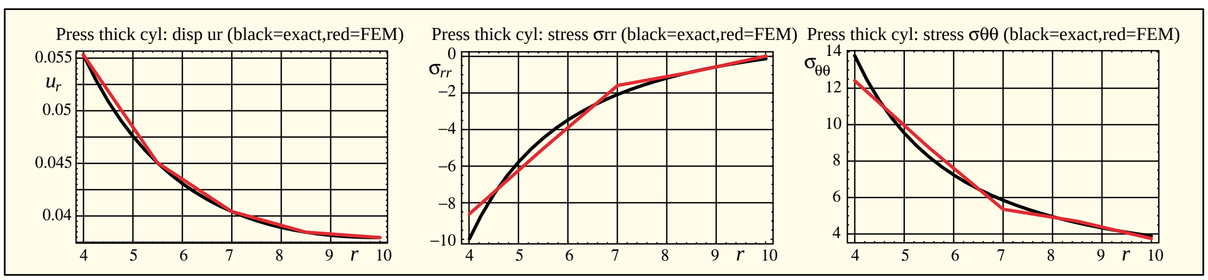

(b) 8 x 1 Mesh of Quad8 Elements, ν = 0:

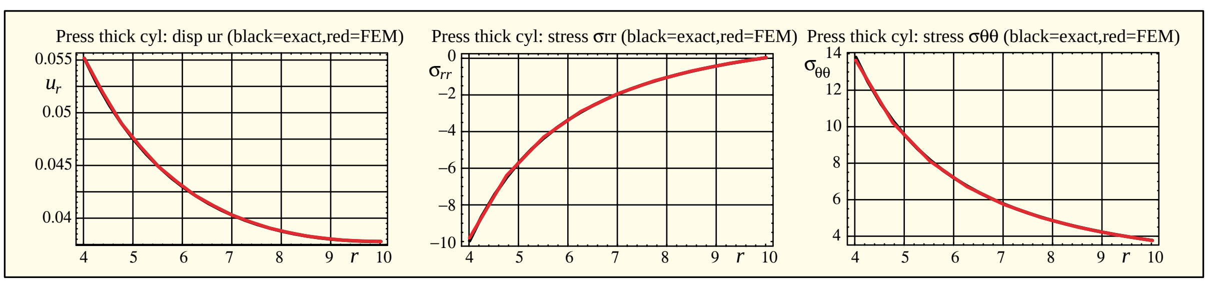

FIGURE 14.7. Pressurized thick cylinder benchmark: r plots of computed versus exact u_r, σ_{rr} and $\sigma_{\theta\theta}$ for Quad8 meshes with $\nu = 0$: (a) 2-element mesh, (b) 8-element mesh.

which exemplifies near-incompressible behavior.[2]

---

[2] Setting $\nu = \frac{1}{2}$ exactly makes the elasticity matrix **E**, as well as **K**, "blow up" and no solution would be obtained.

Computed solution

node	r-disp	z-disp	sigma-rr	sigma-zz	sigma-θθ	sigma-rz	r-force	z-force
1	0.0170	0.0000	174.2420	176.2850	179.0340	0.0000	40.0000	-207.7300
2	0.0170	0.0000	174.2420	176.2850	179.0340	0.0000	40.0000	207.7300
3	0.0124	0.0000	-38.6784	-37.0706	-35.6114	0.0000	0.0000	55.3264
4	0.0124	0.0000	-38.6784	-37.0706	-35.6114	0.0000	0.0000	-55.3264
5	0.0097	0.0000	-14.2501	-13.2835	-12.3703	0.0000	0.0000	21.8783
6	0.0097	0.0000	-14.2501	-13.2835	-12.3703	0.0000	0.0000	-21.8783
7	0.0080	0.0000	-6.2986	-5.6522	-5.0285	0.0000	0.0000	7.4675
8	0.0080	0.0000	-6.2986	-5.6522	-5.0285	0.0000	0.0000	-7.4675
9	0.0068	0.0000	-20.6648	-20.1323	-19.6805	0.0000	0.0000	43.2181
10	0.0068	0.0000	-20.6648	-20.1323	-19.6805	0.0000	0.0000	-43.2181

Exact (Lame) solution

node	r-disp	z-disp	sigma-rr	sigma-zz	sigma-θθ	sigma-rz
1	0.0714	0.0000	-10.0000	1.9010	13.8095	0.0000
2	0.0714	0.0000	-10.0000	1.9010	13.8095	0.0000
3	0.0519	0.0000	-4.3920	1.9010	8.2015	0.0000
4	0.0519	0.0000	-4.3920	1.9010	8.2015	0.0000
5	0.0408	0.0000	-1.9825	1.9010	5.7920	0.0000
6	0.0408	0.0000	-1.9825	1.9010	5.7920	0.0000
7	0.0336	0.0000	-0.7316	1.9010	4.5411	0.0000
8	0.0336	0.0000	-0.7316	1.9010	4.5411	0.0000
9	0.0286	0.0000	0.0000	1.9010	3.8095	0.0000
10	0.0286	0.0000	0.0000	1.9010	3.8095	0.0000

FIGURE 14.8. Pressurized thick cylinder benchmark: computed and exact nodal solution for 4-element Quad4 mesh with Poisson ratio $\nu = 0.499$. The mesh is that shown in Figure 14.2(b).

(a) 4 x 1 Mesh of Quad4 Elements, ν = 0.499:

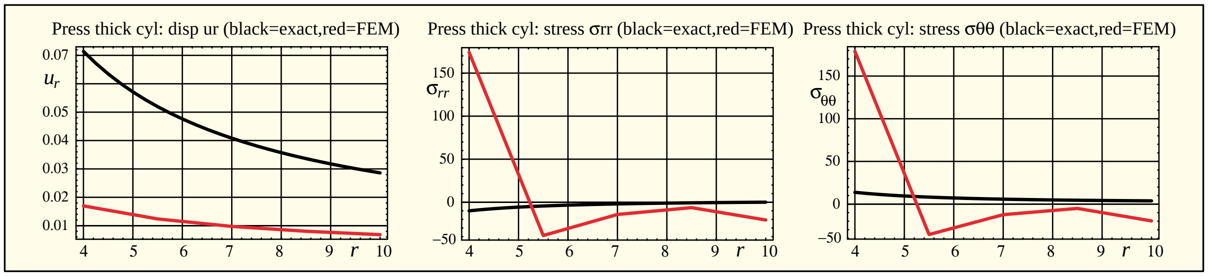

(b) 16 x 1 Mesh of Quad4 Elements, ν = 0.499:

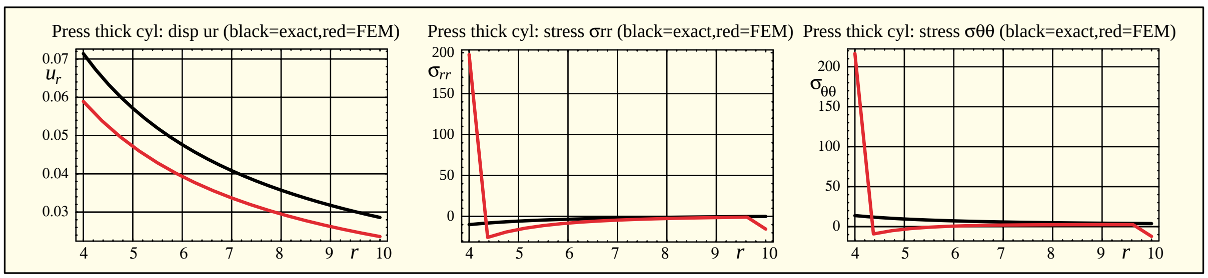

FIGURE 14.9. Pressurized thick cylinder benchmark: r plots of computed versus exact u_r, σ_{rr} and $\sigma_{\theta\theta}$ for Quad4 meshes with $\nu = 0.499$: (a) 4-element mesh, (b) 16-element mesh.

Computed and exact nodal values are tabulated in Figure 14.8. Radial displacements u_r, radial stresses σ_{rr} and hoop stresses $\sigma_{\theta\theta}$ are graphically compared over $a \le r \le b$ with the exact solution in Figure 14.9(a). Serious deficiencies can be observed. The radial displacement u_r has the right profile but is only about 20% of the correct values; for example at $r = a$ the computed value is 0.0170 versus 0.0714. All stress components violently oscillate as one approaches the inner boundary, and the values taken there are nonsensical. For example $\sigma_{rr} \approx 174$ at $r = a$ whereas it

Computed solution

node	r-disp	z-disp	sigma-rr	sigma-zz	sigma-θθ	sigma-rz	r-force	z-force
1	0.0714	0.0000	−8.6085	1.9010	12.4181	0.0000	13.3333	−3.8019
2	0.0714	0.0000	−8.6085	1.9010	12.4181	0.0000	53.3333	0.0000
3	0.0714	0.0000	−8.6085	1.9010	12.4181	0.0000	13.3333	3.8019
4	0.0519	0.0000	−4.8980	1.9010	8.7075	0.0000	0.0000	−20.9105
5	0.0519	0.0000	−4.8980	1.9010	8.7075	0.0000	0.0000	20.9105
6	0.0408	0.0000	−1.4820	1.9010	5.2916	0.0000	0.0000	−13.3067
7	0.0408	0.0000	−1.4820	1.9010	5.2916	0.0000	0.0000	0.0000
8	0.0408	0.0000	−1.4820	1.9010	5.2916	0.0000	0.0000	13.3067
9	0.0336	0.0000	−0.8163	1.9010	4.6259	0.0000	0.0000	−32.3162
10	0.0336	0.0000	−0.8163	1.9010	4.6259	0.0000	0.0000	32.3162
11	0.0286	0.0000	0.1441	1.9010	3.6655	0.0000	0.0000	−9.5048
12	0.0286	0.0000	0.1441	1.9010	3.6655	0.0000	0.0000	0.0000
13	0.0286	0.0000	0.1441	1.9010	3.6655	0.0000	0.0000	9.5048

Exact (Lame) solution

node	r-disp	z-disp	sigma-rr	sigma-zz	sigma-θθ	sigma-rz
1	0.0714	0.0000	−10.0000	1.9010	13.8095	0.0000
2	0.0714	0.0000	−10.0000	1.9010	13.8095	0.0000
3	0.0714	0.0000	−10.0000	1.9010	13.8095	0.0000
4	0.0519	0.0000	−4.3920	1.9010	8.2015	0.0000
5	0.0519	0.0000	−4.3920	1.9010	8.2015	0.0000
6	0.0408	0.0000	−1.9825	1.9010	5.7920	0.0000
7	0.0408	0.0000	−1.9825	1.9010	5.7920	0.0000
8	0.0408	0.0000	−1.9825	1.9010	5.7920	0.0000
9	0.0336	0.0000	−0.7316	1.9010	4.5411	0.0000
10	0.0336	0.0000	−0.7316	1.9010	4.5411	0.0000
11	0.0286	0.0000	0.0000	1.9010	3.8095	0.0000
12	0.0286	0.0000	0.0000	1.9010	3.8095	0.0000
13	0.0286	0.0000	0.0000	1.9010	3.8095	0.0000

FIGURE 14.10. Pressurized thick cylinder benchmark: computed and exact nodal solution for 2-element Quad8 mesh with Poisson ratio $\nu = 0.499$. The mesh is that shown in Figure 14.2(b).

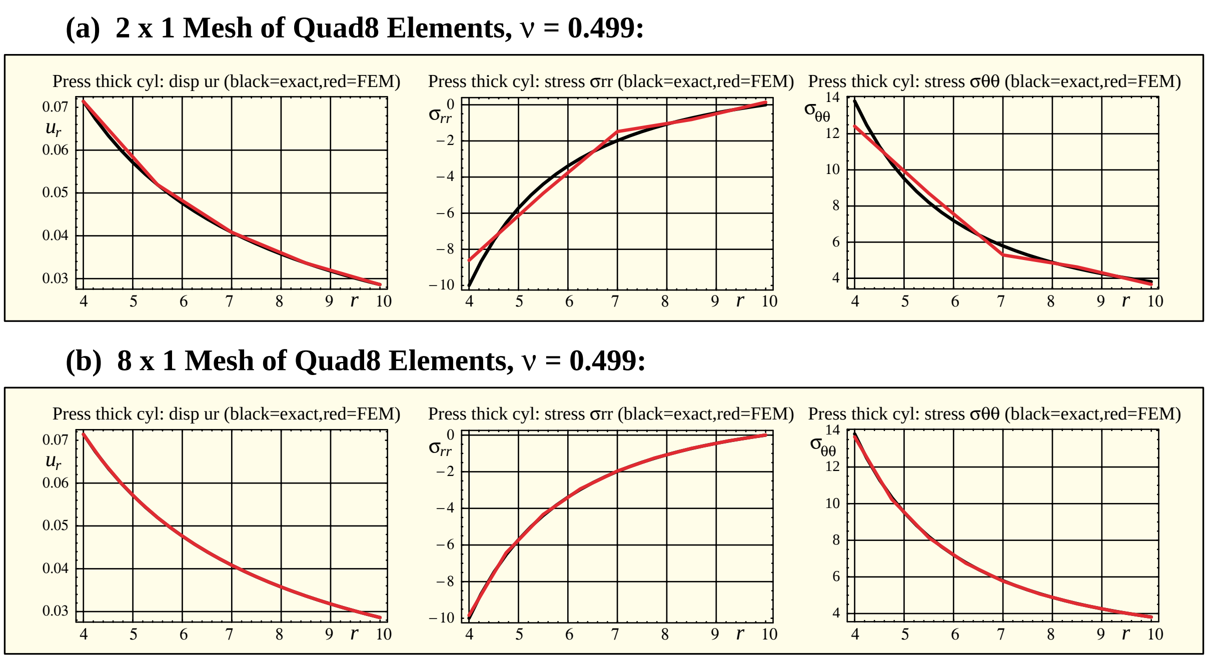

FIGURE 14.11. Pressurized thick cylinder benchmark: r plots of computed versus exact u_r, σ_{rr} and $\sigma_{\theta\theta}$ for Quad8 meshes with $\nu = 0.499$: (a) 2-element mesh, (b) 8-element mesh.

should be $-p = -10$, so it even has the wrong sign.

The number of elements is then increased to 16. Results are compared with the exact solution in Figure 14.9(b). The displacements u_r are more reasonable although still visibly off. The violent

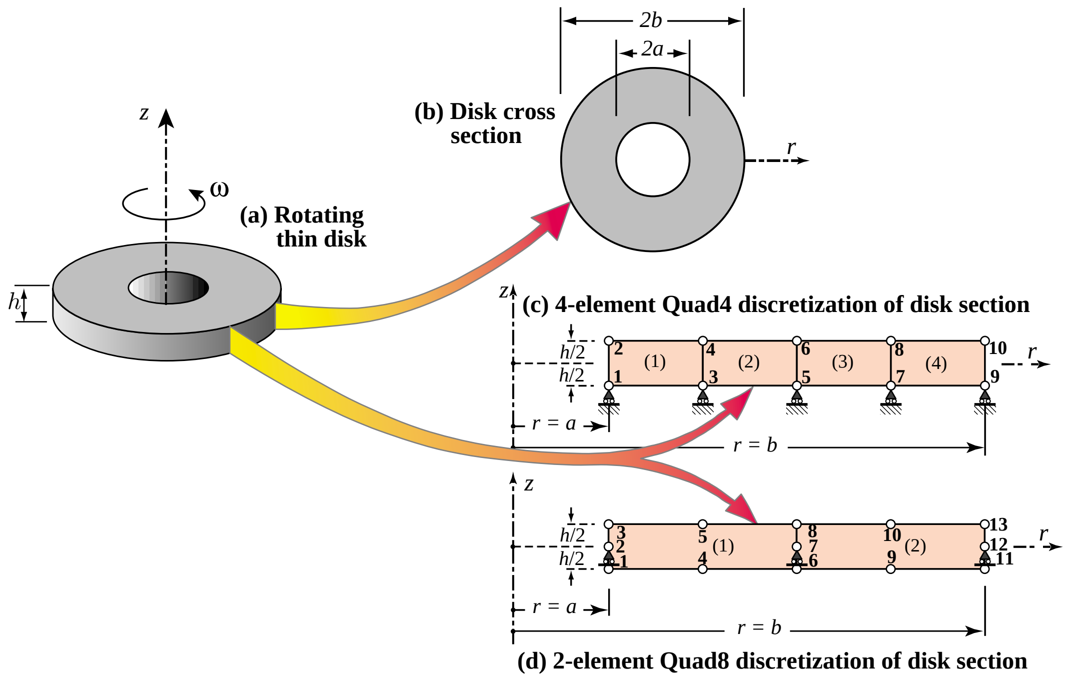

FIGURE 14.12. Rotating thin disk benchmark problem.

stress oscillation moves closer to the inner boundary, and results there are even worse than with the 4-element mesh. A minor stress oscillation can be observed at the outer boundary.

Changing the FEM model to `Quad8` with reduced integration makes a big difference. For a 2-element mesh like that shown in Figure 14.2(c), computed and exact nodal values are tabulated in Figure 14.10. Radial displacements u_r, radial stresses σ_{rr} and hoop stresses $\sigma_{\theta\theta}$ are graphically compared over $a \le r \le b$ with the exact solution in Figure 14.11(a). As can be seen the model retains nodal exactness for displacements. Neither volumetric locking nor stress oscillations are observed, and the stresses are well predicted everywhere.

The number of elements is then increased to 8. Results are compared with the exact solution in Figure 14.11(b). The agreement with the exact solution is excellent.

In summary, the `Quad4` model is useless for near-incompressible material in this benchmark and, in general, when modeling bulky axisymmetric solids.[3]. On the other hand, the rediced integration `Quad8` can be strongly recommended for those problems.

Remark 14.1. If `Quad8` is processed by a 3×3 integration Gauss rule, which represents full integration, volumetric locking reappears. So going from `Quad4` to `Quad8` is not sufficient: the integration rule makes a significant difference for near-incompressible behavior.

§14.2. Benchmark Example 2: Rotating Thin Disk

The second benchmark problem is a hollow, thin circular disk of thickness h, inner radius a and outer radius b, which spins about the z axis with constant angular frequency ω. The material is

[3] The effect of volumetric locking is not so pronounced in the other two benchmarks because the plane strain condition is replaced by one of plane stress.

isotropic with elastic modulus E and Poisson's ratio ν and mass density ρ. The r axis is placed in the disk midplane. See Figure 14.12(a,b).

The FEM discretizations pictured in Figure 14.12(c,d) mimic those used in the pressurized thick cylinder benchmark, as shown in Figure 14.2(b,c). The number of elements in the radial direction is 4 and 16 for `Quad4` and 2 and 8 for `Quad8`, respectively. Only one element is used in the axial direction. Nodes are allowed to move radially. Unlike the previous benchmark, however, movement in the axial (z) direction is permitted to allow for disk thickness contraction due to Poisson ratio. This motion is accomodated by constraining nodes in one of the constant-z surfaces to be on rollers as shown in Figure 14.12(c,d). All other nodes are left free. The only load is a centrifugal body force acting along r: $b_r = \rho\,\omega^2\, r$ while $b_z = 0$.

§14.2.1. Exact Solution

The exact stress distribution for a condition of plane stress in the z direction is [4]

$$\begin{aligned}\sigma_{rr} &= \rho\,\omega^2\, r\,\frac{3+\nu}{8}\left(b^2+a^2-\frac{a^2\,b^2}{r^2}-r^2\right),\\ \sigma_{\theta\theta} &= \rho\,\omega^2\, r\,\frac{3+\nu}{8}\left(b^2+a^2+\frac{a^2\,b^2}{r^2}-\frac{(1+3\nu)r^2}{(3+\nu)}\right),\end{aligned}\tag{14.3}$$

others zero. Recovering strains from (14.3) and integrating yields the displacements

$$\begin{aligned}u_r &= \rho\,\omega^2\,\frac{a^2(3+\nu)\big(r^2(1-\nu)+b^2(1+\nu)\big)+r^2(1-\nu)\big(b^2(3+\nu)-r^2(1+\nu)\big)}{8\,E\,r},\\ u_z &= \rho\,\omega^2\, z\,\nu\,\frac{(1-\nu-2\nu^2)\big(2r^2(1+\nu)-a^2(3+\nu)-b^2(3+\nu)\big)}{4E\,(1+3\nu)}.\end{aligned}\tag{14.4}$$

Notice that $u_z = 0$ at $z = 0$, which removes the axial rigid body motion. If $\nu = 0$, $u_z = 0$ as may be expected, whereas if $\nu = \frac{1}{2}$, $u_z = \frac{1}{2}\rho\,\omega^2\, z$.

§14.2.2. Driver Script

The *Mathematica* driver script listed in Figure 14.13 accepts both 4-node and 8-node quad elements. Note that geometric, constitutive and discretization properties are declared at the top to make parametrization simpler. To set the element type it is sufficient to declare `etype` in the second line of the script to be either `"Quad4"` or `"Quad8"`. The number of elements along the radial and axial directions: N_{er} and N_{ez}, are parametrized by the values assigned to `Ner` and `Nez`, respectively. The latter is assumed to be 1.

If the element type is `"Quad4"` a regular mesh is generated by modules `GenQuad4NodeCoordinates` and `GenQuad4ElemNodes`, described in the previous Chapter. If the element type is `Quad8` the generation modules invoked are `GenQuad8NodeCoordinates` and `GenQuad8ElemNodes`. the element type is `"Quad8"`. Pressure lumping to the nodes on the inner radius $r = a$ depends on element type. The body force field is specified at the 4 element corner nodes, regardless of whether the element type is `Quad4` or `Quad8`.

[4] Taken from S. Timoshenko and J. N. Goodier, *Theory of Elasticity*, McGraw-Hill, 2nd ed., 1951, Chapter 4. If $a \to 0$ the solution has a removable singularity at $r = 0$.

```
ClearAll[Em,ν,a,b,h,Kfac,ρ,| ,Ner,Nez,numer];
Em=1000.; ν=N[1/3];  Ner=4; Nez=1; etype="Quad4";
Kfac=1; a=4; b=10; h=1; aspect=h/(b-a); ρ=3.0; ω=0.5;
numer=True;

(*  Define FEM model *)

MeshCorners=N[{{a,0},{b,0},{b,h},{a,h}}];
If [etype=="Quad4",
    NodeCoordinates=GenQuad4NodeCoordinates[MeshCorners,Ner,Nez];
    ElemNodes=  GenQuad4ElemNodes[Ner,Nez]];
If [etype=="Quad8",
    NodeCoordinates=GenQuad8NodeCoordinates[MeshCorners,Ner,Nez];
    ElemNodes=  GenQuad8ElemNodes[Ner,Nez]];
numnod=Length[NodeCoordinates]; numele=Length[ElemNodes];
ElemType=      Table[etype,{numele}];
ElemMaterial=  Table[{Em,ν},{numele}];
ElemBodyForces=Table[{0,0},{numele}];
For [e=1,e<=numele,e++, enl=ElemNodes[[e]];
     ncoor=Table[NodeCoordinates[[enl[[i]]]],{i,4}];
     {{r1,z1},{r2,z2},{r3,z3},{r4,z4}}=ncoor;
     ElemBodyForces[[e]]=ρ*| ^2*{{r1,0},{r2,0},{r3,0},{r4,0}}];
FreedomTags=FreedomValues=Table[{0,0},{numnod}];
If [etype=="Quad4",
    For [n=1,n<=numnod-Nez,n=n+Nez+1, FreedomTags[[n]]={0,1}]];
If [etype=="Quad8",
    For [n=1,n<=numnod-2*Nez,n=n+3*Nez+2, FreedomTags[[n+1]]={0,1}]];
ElemTractionForces={}; DefaultOptions={True};
(* Model definition print statements removed to shorten script *)
Plot2DElementsAndNodes[NodeCoordinates,ElemNodes,aspect,
    "Rotating disk mesh",True,True];

(*  Solve problem and print results *)

{NodeDisplacements,NodeForces,NodeStresses}=RingAnalysisDriver[
    NodeCoordinates,ElemType,ElemNodes,
    ElemMaterial,ElemBodyForces,ElemTractionForces,
    FreedomTags,FreedomValues,DefaultOptions];
PrintRingAnalysisSolution[NodeDisplacements,NodeForces,
    NodeStresses,"Computed solution",{}];
{ExactNodeDisplacements,ExactNodeStresses}=
    ExactSolution[NodeCoordinates,{a,b,h},{Em,ν,ρ   | ,
     "RotatingThinDisk",numer];
PrintRingNodeDispStresses[ExactNodeDisplacements,
    ExactNodeStresses,"Exact solution",{}];

(* Contour plots of stress distributions *)

legend={(a+b)/2,0.75*h}; whichones={True,False,True,False};
ContourPlotStresses[NodeCoordinates,ElemNodes,NodeStresses,
  whichones,True,{},legend,aspect];

(* Radial plots comparing FEM vs exact solutions *)

pwhat={"ur","σrr","σzz","σθθ"};
For [ip=1,ip<=Length[pwhat],ip++, what=pwhat[[ip]];
     RadialPlotFEMvsExact[etype,NodeCoordinates,NodeDisplacements,
       NodeStresses,{a,b,h},{Em,ν,ρ},| ,{Ner,Nez},
       "RotatingThinDisk",what,0,numer]  ];
```

FIGURE 14.13. Script for rotating disk benchmark problem.

Computed solution

node	r–disp	z–disp	sigma–rr	sigma–zz	sigma–θθ	sigma–rz	r–force	z–force
1	0.2567	0.0000	12.2963	2.3994	67.8220	−0.7835	5.7305	−0.5185
2	0.2547	−0.0243	12.6637	2.3936	67.4372	0.7073	5.7305	0.0000
3	0.2401	0.0000	7.7905	−0.6290	45.3527	−0.5037	17.2266	1.3833
4	0.2387	−0.0183	8.1077	−0.5589	45.2458	0.5598	17.2266	0.0000
5	0.2354	0.0000	9.2003	−0.6720	36.1805	−0.4128	27.7734	−1.3919
6	0.2343	−0.0158	9.1420	−0.7594	35.9764	0.4104	27.7734	0.0000
7	0.2322	0.0000	6.1607	0.0342	29.2155	−0.4599	40.8516	0.6446
8	0.2309	−0.0118	6.0606	−0.0697	29.0039	0.4653	40.8516	0.0000
9	0.2246	0.0000	2.9120	0.3871	23.4411	−0.4071	25.4180	−0.1175
10	0.2235	−0.0084	2.9721	0.3768	23.3500	0.4331	25.4180	0.0000

Exact (plane stress) solution

node	r–disp	z–disp	sigma–rr	sigma–zz	sigma–θθ	sigma–rz
1	0.2580	0.0000	0.0000	0.0000	64.5000	0.0000
2	0.2580	−0.0048	0.0000	0.0000	64.5000	0.0000
3	0.2403	0.0000	10.2679	0.0000	47.1071	0.0000
4	0.2403	−0.0043	10.2679	0.0000	47.1071	0.0000
5	0.2358	0.0000	10.7334	0.0000	37.2666	0.0000
6	0.2358	−0.0036	10.7334	0.0000	37.2666	0.0000
7	0.2327	0.0000	6.7515	0.0000	29.6235	0.0000
8	0.2327	−0.0027	6.7515	0.0000	29.6235	0.0000
9	0.2250	0.0000	0.0000	0.0000	22.5000	0.0000
10	0.2250	−0.0017	0.0000	0.0000	22.5000	0.0000

FIGURE 14.14. Rotating disk benchmark: computed results and exact solution for 4-element `Quad4` mesh, with Poisson ratio $\nu = 1/3$.

(a) 4 x 1 Mesh of Quad4 Elements, ν = 1/3:

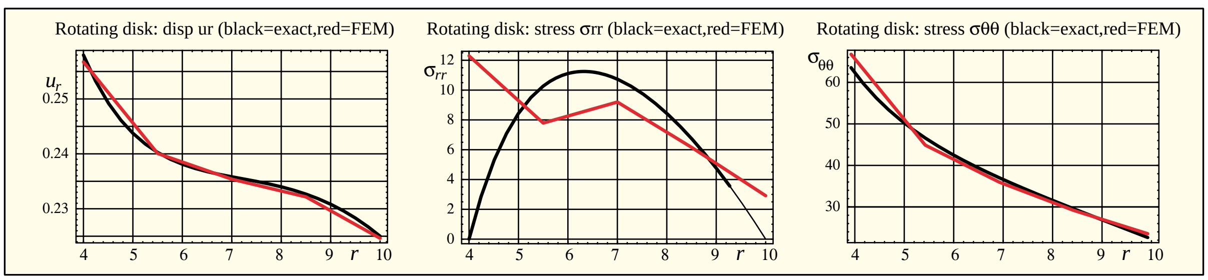

(b) 16 x 1 Mesh of Quad4 Elements, ν = 1/3:

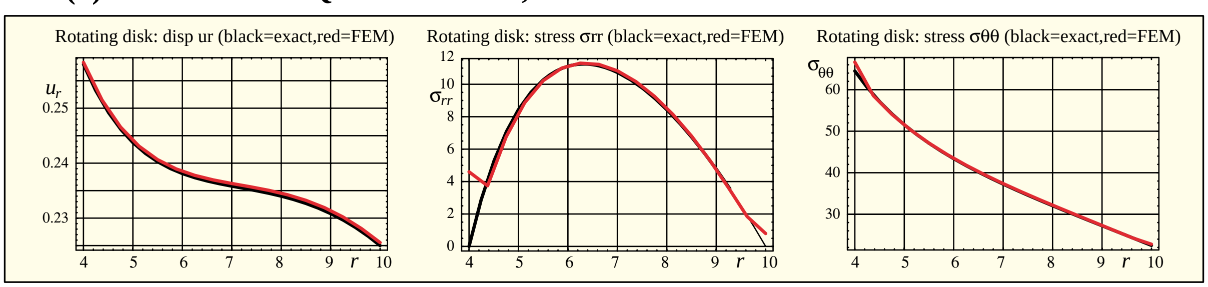

FIGURE 14.15. Rotating disk benchmark: radial plots of u_r, σ_{rr} and $\sigma_{\theta\theta}$ for 4-element and 16-element `Quad4`, with Poisson ratio $\nu = 1/3$.

§14.2.3. Numerical Results

The results presented here were computed for $a = 4$, $b = 10$, $h = 1$, $p = 10$, $E = 1000$, $\nu = 1/3$, two element types, and two radial discretizations for each type.

The script of Figure 14.13 specifically sets `etype="Quad4"`, `Ner=4` and $\nu = 1/3$. The mesh is actually that pictured in Figure 14.12(c). Computed and exact nodal values are tabulated in Figure

Computed solution

node	r-disp	z-disp	sigma-rr	sigma-zz	sigma-θθ	sigma-rz	r-force	z-force
1	0.2577	0.0108	4.2728	0.0000	61.2000	0.0000	-6.8437	0.0000
2	0.2579	0.0000	4.2728	0.0000	61.2000	0.0000	19.1250	0.0000
3	0.2577	-0.0108	4.2728	0.0000	61.2000	0.0000	-6.8437	0.0000
4	0.2401	0.0096	8.7239	0.0000	48.2944	0.0000	23.2500	0.0000
5	0.2401	-0.0096	8.7239	0.0000	48.2944	0.0000	23.2500	0.0000
6	0.2356	0.0080	12.5046	0.0000	36.2225	0.0000	-20.0625	0.0000
7	0.2358	0.0000	12.5046	0.0000	36.2225	0.0000	75.7500	0.0000
8	0.2356	-0.0080	12.5046	0.0000	36.2225	0.0000	-20.0625	0.0000
9	0.2324	0.0061	6.3024	0.0000	29.7056	0.0000	54.7500	0.0000
10	0.2324	-0.0061	6.3024	0.0000	29.7056	0.0000	54.7500	0.0000
11	0.2247	0.0037	0.7706	0.0000	22.3550	0.0000	-12.0937	0.0000
12	0.2251	0.0000	0.7706	0.0000	22.3550	0.0000	61.1250	0.0000
13	0.2247	-0.0037	0.7706	0.0000	22.3550	0.0000	-12.0937	0.0000

Exact (plane stress) solution

node	r-disp	z-disp	sigma-rr	sigma-zz	sigma-θθ	sigma-rz
1	0.2580	0.0000	0.0000	0.0000	64.5000	0.0000
2	0.2580	-0.0024	0.0000	0.0000	64.5000	0.0000
3	0.2580	-0.0048	0.0000	0.0000	64.5000	0.0000
4	0.2403	0.0000	10.2679	0.0000	47.1071	0.0000
5	0.2403	-0.0043	10.2679	0.0000	47.1071	0.0000
6	0.2358	0.0000	10.7334	0.0000	37.2666	0.0000
7	0.2358	-0.0018	10.7334	0.0000	37.2666	0.0000
8	0.2358	-0.0036	10.7334	0.0000	37.2666	0.0000
9	0.2327	0.0000	6.7515	0.0000	29.6235	0.0000
10	0.2327	-0.0027	6.7515	0.0000	29.6235	0.0000
11	0.2250	0.0000	0.0000	0.0000	22.5000	0.0000
12	0.2250	-0.0008	0.0000	0.0000	22.5000	0.0000
13	0.2250	-0.0017	0.0000	0.0000	22.5000	0.0000

FIGURE 14.16. Rotating disk benchmark: computed results and exact solution for 2-element `Quad8` mesh, with Poisson ratio $\nu = 1/3$.

(a) 2 x 1 Mesh of Quad8 Elements, ν = 1/3:

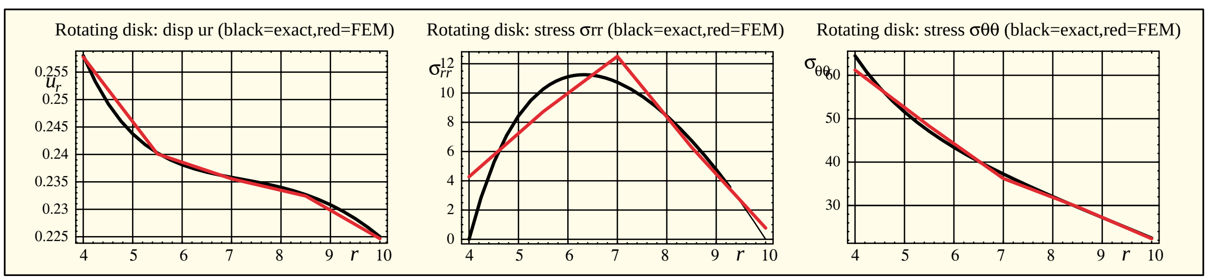

(b) 8 x 1 Mesh of Quad8 Elements, ν = 1/3:

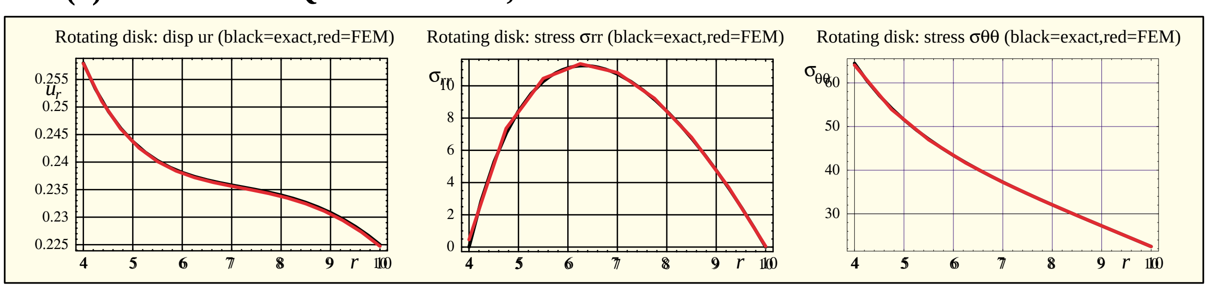

FIGURE 14.17. Rotating disk benchmark: radial plots of u_r, σ_{rr} and $\sigma_{\theta\theta}$ for 2-element and 8-element `Quad8` meshes, with Poisson ratio $\nu = 1/3$.

14.14. Radial displacements u_r, radial stresses σ_{rr} and hoop stresses $\sigma_{\theta\theta}$ are graphically compared over $a \le r \le b$ with the exact solution in Figure 14.15(a).

As can be seen u_r and $\sigma_{\theta\theta}$ are satisfactorily predicted. The radial stress, however, is way off, especially at the inner and outer boundaries, at which it should be zero. This is again a consequence of the impossibility of doing interelement stress averaging there. For this low-order model the variation of σ_{rr} in the r direction is limited to be constant within the element.

Increasing `Ner` to 16 gives a solution that is compared with the exact one in Figure 14.15(b). Both u_r and $\sigma_{\theta\theta}$ are correct to at least 3 places. The notable flaw is the discrepancy of σ_{rr} at both boundaries. Again this is a consequence of lack of interelement averaging. Away from the hole σ_{rr} agrees with the exact solution to satisfactory accuracy.

The analysis is then redone with the 8-node quadrilateral `Quad8` with reduced (2×2) integration. To make a fair comparison with `Quad4`, the `Quad8` meshes contain half the elements: 2 and 8, respectively, which results in a similar number of nodes.

The results of running `Quad8` with `Ner=2` are tabulated in Figure 14.16. Radial displacements u_r, radial stresses σ_{rr} and hoop stresses $\sigma_{\theta\theta}$ are graphically compared over $a \le r \le b$ with the exact solution in Figure 14.17(a). This element is supposed to be nodally exact for one-dimensional problems, and indeed the computed and exact u_r may be verified to agree numerically to 15 places at all nodes. The hoop stress should be also nodally exact since $\sigma_{\theta\theta} = E\, u_r/r$, but the extrapolation from Gauss points introduces discrepancies. The computed radial stress σ_{rr} is as good as can be expected from a linear variation over the element.

Running `Quad8` with `Ner=8` give the results plotted in Figure 14.17(b). Again the displacements are nodally exact. Both σ_{rr} and $\sigma_{\theta\theta}$ agree everywhere with the exact solution at plot accuracy.

Rerunning these cases for a Poisson ratio close to $\frac{1}{2}$ shows deteriorartion of `Quad4` accuracy, but not so dramatic as that experienced in the pressurized thick cylinder benchmark. This indicates that volumetric locking is less of a problem in this case, as could be expected since the plane stress condition allows lateral expansion and contraction.

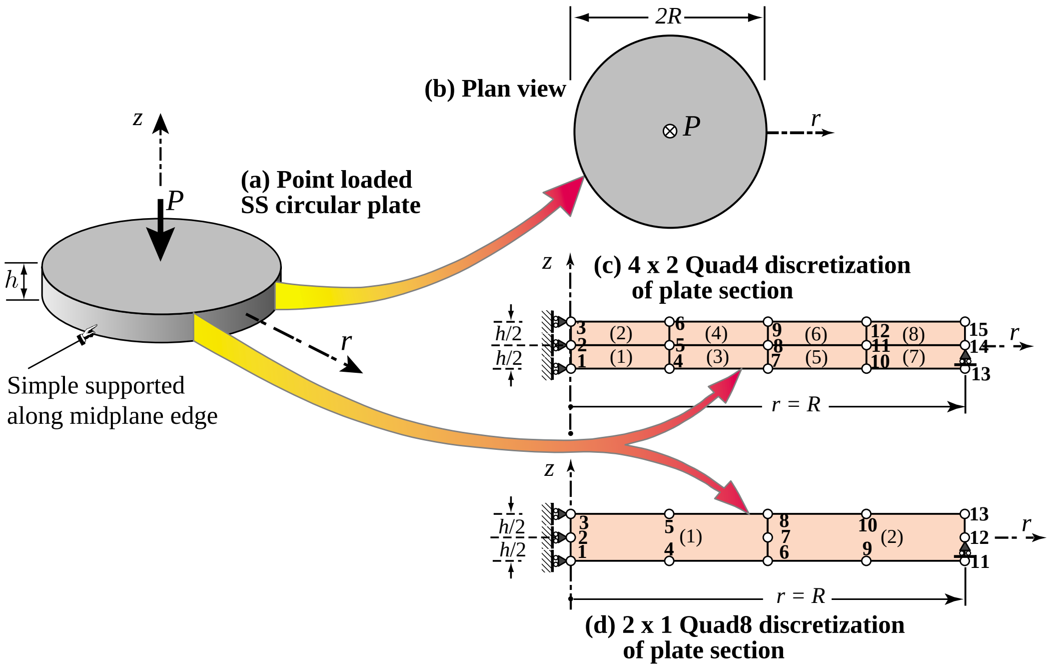

FIGURE 14.18. Point-loaded circular plate bending benchmark problem.

§14.3. Benchmark 3: Point Loaded SS Circular Plate Bending

The third benchmark problem is a simply-supported (SS) circular plate bent by a lateral point load. The plate has radius R and thickness h. The point load of magnitude P acts downward at the plate center. The material is isotropic with elastic modulus E and Poisson's ratio ν. See Figure 14.18(a,b) for the problem definition.

Two FEM discretizations are pictured in Figure 14.18(c,d).

For the `Quad4` element type 4×2 and 16×2 discretizations are used, whereas for `Quad8` the meshes are 2×1 and 8×1. The reason for selecting 2 elements along z for the `Quad4` discretization is that it provides nodes at the midplane $z = 0$, allowing a midplane-symmetric specification of the simple supported BC at $r = R$.

For the `Quad8` discretization one element along z is suffiucient since several midnodes are available on the midplane. Nodes are allowed to move in the z direction except those on the midplane $z = 0$ at $r = R$. The 3 nodes at $r = 0$ must be constrained against radial motion. The resulting support conditions are shown in Figure 14.18(c,d). The central point load P is divided by 2Π since $K_{fac} = 1$ and then appropriately lumped to the 3 nodes on the z axis.

§14.3.1. Exact Solution

The exact solution[5] for a Kirchhoff plate model of this problem[6] gives the bending moments and associated stresses as

$$M_{rr} = \frac{P}{4\pi}(1+\nu)\,\log\frac{R}{r}, \quad \sigma_{rr} = 12 M_{rr} z/h^3,$$
$$M_{\theta\theta} = \frac{P}{4\pi}\left[(1+\nu)\,\log\frac{R}{r} + 1 - \nu\right], \quad \sigma_{\theta\theta} = 12 M_{\theta\theta} z/h^3, \tag{14.5}$$

Other stress components are zero. Moments and stresses given by (14.5) become infinite at $r = 0$ under the point load, so when comparing to a FEM solution r is limited to $r \le r_{truc} = R/1000$ to avoid blow-ups. The stresses at the upper and lower plate surfaces are $\sigma_{rr} = \pm 12 M_{rr}(h/2)/h^3 = \pm 6 M_{rr}/h^2$ and $\sigma_{\theta\theta} = \pm 12 M_{\theta\theta}(h/2)/h^3 = \pm 6 M_{\theta\theta}/h^2$. The transverse displacement is

$$u_z = -\frac{P}{16\pi D}\left[\frac{3+\nu}{1+\nu}(R^2 - r^2) + 2r^2 \log\frac{r}{R}\right], \tag{14.6}$$

where $D = Eh^3/(12(1-\nu^2))$ is the plate rigidity. Note that u_z does not depend on z, which follows from the Kirchhoff thin plate theory assumptions. Also u_z is finite at $r = 0$ because $\lim_{r\to 0} r^2 \,\log(r/R) = 0$. The radial displacement is given by

$$u_r = -z\,\frac{\partial u_z}{\partial r} = \frac{P}{8\pi D}\left(\frac{3+\nu}{1+\nu} - 1 - 2\log\frac{r}{R}\right) r\,z, \tag{14.7}$$

which also vanishes at $r = 0$.

§14.3.2. Driver Script

The driver script for the point-loaded circular plate benchmark is listed in Figure 14.19. This is similar to the previous scripts except for the use of 2 elements along the thickness (the axial or z direction) if the element type is `Quad4`. The central force is scaled by $K_{fac}/(2\pi) = 1/(2\pi)$ and distributed to the 3 nodes at $r = 0$.

---

[5] Taken from S. Timoshenko and S. Woinowsky-Krieger, *Theory of Plates and Shells*, McGraw-Hill, 2nd ed., 1959, Ch. 2.

[6] The Kirchhoff model assumes that the plate is thin in the sense that $h << R$, but not so thin as to become a membrane.

```
ClearAll[Em,ν,a,b,h,Kfac,ρ,| ,Ner,Nez,numer];
Em=1000.; ν=N[1/3];  Ner=4; Nez=1; etype="Quad4";
Kfac=1; a=4; b=10; h=1; aspect=h/(b-a); ρ=3.0; | =0.5;
numer=True;

(*  Define FEM model *)

MeshCorners=N[{{a,0},{b,0},{b,h},{a,h}}];
If [etype=="Quad4",
    NodeCoordinates=GenQuad4NodeCoordinates[MeshCorners,Ner,Nez];
    ElemNodes=  GenQuad4ElemNodes[Ner,Nez]];
If [etype=="Quad8",
    NodeCoordinates=GenQuad8NodeCoordinates[MeshCorners,Ner,Nez];
    ElemNodes=  GenQuad8ElemNodes[Ner,Nez]];
numnod=Length[NodeCoordinates]; numele=Length[ElemNodes];
ElemType=      Table[etype,{numele}];
ElemMaterial=  Table[{Em,ν},{numele}];
ElemBodyForces=Table[{0,0},{numele}];
For [e=1,e<=numele,e++, enl=ElemNodes[[e]];
     ncoor=Table[NodeCoordinates[[enl[[i]]]],{i,4}];
     {{r1,z1},{r2,z2},{r3,z3},{r4,z4}}=ncoor;
     ElemBodyForces[[e]]=ρ*| ^2*{{r1,0},{r2,0},{r3,0},{r4,0}}];
FreedomTags=FreedomValues=Table[{0,0},{numnod}];
If [etype=="Quad4",
    For [n=1,n<=numnod-Nez,n=n+Nez+1, FreedomTags[[n]]={0,1}]];
If [etype=="Quad8",
    For [n=1,n<=numnod-2*Nez,n=n+3*Nez+2, FreedomTags[[n+1]]={0,1}]];
ElemTractionForces={}; DefaultOptions={True};
(* Print model definition statements removed to shorten script *)
Plot2DElementsAndNodes[NodeCoordinates,ElemNodes,aspect,
    "Rotating disk mesh",True,True];

(*  Solve problem and print results *)

{NodeDisplacements,NodeForces,NodeStresses}=RingAnalysisDriver[
    NodeCoordinates,ElemType,ElemNodes,
    ElemMaterial,ElemBodyForces,ElemTractionForces,
    FreedomTags,FreedomValues,DefaultOptions];
PrintRingAnalysisSolution[NodeDisplacements,NodeForces,
    NodeStresses,"Computed solution",{}];
{ExactNodeDisplacements,ExactNodeStresses}=
    ExactSolution[NodeCoordinates,{a,b,h},{Em,ν,ρ},| ,
     "RotatingThinDisk",numer];
PrintRingNodeDispStresses[ExactNodeDisplacements,
    ExactNodeStresses,"Exact solution",{}];

(*  Contour plot of stress distributions *)

legend={(a+b)/2,0.75*h}; whichones={True,False,True,False};
ContourPlotStresses[NodeCoordinates,ElemNodes,NodeStresses,
  whichones,True,{},legend,aspect];

(* Radial plots comparing FEM vs exact solution *)

pwhat={"ur","σrr","σzz","σθθ"};
For [ip=1,ip<=Length[pwhat],ip++, what=pwhat[[ip]];
     RadialPlotFEMvsExact[etype,NodeCoordinates,NodeDisplacements,
       NodeStresses,{a,b,h},{Em,ν,ρ},| ,{Ner,Nez},
       "RotatingThinDisk",what,0,numer]  ];
```

FIGURE 14.19. Script for point loaded circular plate benchmark problem.

§14.3.3. Numerical Results

The numerical results presented here were computed for $R = 10$, $h = 1$, $E = 1000$, $\nu = 1/3$ and $P = 10$, two element types, and two discretizations for each type.

The script of Figure 14.19 specifically sets `etype="Quad4"`, `Ner=4`, `Nez=2` and $\nu = 1/3$. The mesh is actually that pictured in Figure 14.18(c). Computed and exact nodal values are tabulated in Figure 14.20. The values shown as "exact" for stresses σ_{rr} and $\sigma_{\theta\theta}$ are actually those evaluated from the Kirchhoff solution (14.6) at $r = R/1000 = 1/100$, since those equations have logarithmic singularities as $r \to 0$. Radial displacements u_r, radial stresses σ_{rr} and hoop stresses $\sigma_{\theta\theta}$ are graphically compared over $a \le r \le b$ with the exact solution in Figure 14.21(a). To avoid plot blow-ups the "exact" solutions are again truncated to that small radius.

The radial displacement has the right shape but is underpredicted. This is a mild case of the so-called "shear locking": a significant amount of element energy is spend in shear, resulting in overstiffness. The effect would get worse if the thickness-to-radius ratio (1/10 for this benchmark) is decreased. Considering the coarse mesh the stress predictions are OK sufficiently away from the plate center, say, for $r > 2$. Evidently the FEM solution has trouble capturing the singularity; for that a refined mesh near the center would be required.

Increasing `Ner` to 16 gives a solution that is compared with the exact one in Figure 14.21(b). Shear locking is alleviated but the transverse displacement is still somewaht underpredicted. The stress distribution away from the center are significantly improved, but the singularity is still poorly captured.

The analysis is then redone with the 8-node quadrilateral `Quad8` with reduced (2×2) integration. To make a fair comparison with `Quad4`, the `Quad8` meshes contain half the elements: 2 and 8, respectively, in the radial direction, and only one in the axial direction.

The results of running `Quad8` with `Ner=2` are tabulated in Figure 14.22. Radial displacements u_r, radial stresses σ_{rr} and hoop stresses $\sigma_{\theta\theta}$ are graphically compared over $a \le r \le b$ with the exact solution in Figure 14.23(a). It can be seen that the transverse displacement u_z is well captured (within about 1%) since this element does not suffer from shear locking. The stress distribution is fine away from the center. Capturing the singularity is obviously difficult with 2 elements and a linear stress variation radially, but the model does a good fitting job.

Running `Quad8` with `Ner=8` give the results plotted in Figure 14.23(b). The fit to both displacements and stresses is good, even fairly close to the singularity. No trace of shear locking is observed.

Rerruning these models with $\nu = 0.499$ (results not shown here) degrades the `Quad4` results further (some volumetric locking adds to the shear locking)but has little effect on the `Quad8` discretization.

Computed solution

node	r-disp	z-disp	sigma-rr	sigma-zz	sigma-θθ	sigma-rz	r-force	z-force
1	0.0000	−0.4227	13.4338	4.1445	13.4338	10.6640	−3.9528	−0.3979
2	0.0000	−0.4251	0.0000	0.0000	0.0000	10.8184	0.0000	−0.7958
3	0.0000	−0.4227	−13.4338	−4.1445	−13.4338	10.6640	3.9528	−0.3979
4	0.0189	−0.3516	10.3857	4.8514	12.4267	−0.7101	0.0000	0.0000
5	0.0000	−0.3530	0.0000	0.0000	0.0000	−0.5780	0.0000	0.0000
6	−0.0189	−0.3516	−10.3857	−4.8514	−12.4267	−0.7101	0.0000	0.0000
7	0.0231	−0.2428	4.0131	2.2300	6.5383	−0.1441	0.0000	0.0000
8	0.0000	−0.2434	0.0000	0.0000	0.0000	−0.0730	0.0000	0.0000
9	−0.0231	−0.2428	−4.0131	−2.2300	−6.5383	−0.1441	0.0000	0.0000
10	0.0244	−0.1222	2.0584	1.2624	4.2986	−0.0619	0.0000	0.0000
11	0.0000	−0.1226	0.0000	0.0000	0.0000	−0.0325	0.0000	0.0000
12	−0.0244	−0.1222	−2.0584	−1.2624	−4.2986	−0.0619	0.0000	0.0000
13	0.0242	0.0003	1.2697	0.9626	3.1253	0.2516	0.0000	0.0000
14	0.0000	0.0000	0.0000	0.0000	0.0000	0.2782	0.0000	1.5915
15	−0.0242	0.0003	−1.2697	−0.9626	−3.1253	0.2516	0.0000	0.0000

Thin plate (Kirchhoff) solution

node	r-disp	z-disp	sigma-rr	sigma-zz	sigma-θθ	sigma-rz
1	0.0000	−0.5305	43.9761	0.0000	47.1592	0.0000
2	0.0000	−0.5305	0.0000	0.0000	0.0000	0.0000
3	0.0000	−0.5305	−43.9761	0.0000	−47.1592	0.0000
4	0.0227	−0.4606	8.8254	0.0000	12.0085	0.0000
5	0.0000	−0.4606	0.0000	0.0000	0.0000	0.0000
6	−0.0227	−0.4606	−8.8254	0.0000	−12.0085	0.0000
7	0.0306	−0.3243	4.4127	0.0000	7.5958	0.0000
8	0.0000	−0.3243	0.0000	0.0000	0.0000	0.0000
9	−0.0306	−0.3243	−4.4127	0.0000	−7.5958	0.0000
10	0.0330	−0.1634	1.8314	0.0000	5.0145	0.0000
11	0.0000	−0.1634	0.0000	0.0000	0.0000	0.0000
12	−0.0330	−0.1634	−1.8314	0.0000	−5.0145	0.0000
13	0.0318	0.0000	0.0000	0.0000	3.1831	0.0000
14	0.0000	0.0000	0.0000	0.0000	0.0000	0.0000
15	−0.0318	0.0000	0.0000	0.0000	−3.1831	0.0000

FIGURE 14.20. Point loaded circular plate benchmark: computed results and exact solution for 4 × 2 Quad4 mesh, with Poisson ratio $\nu = 1/3$.

(a) 4 x 2 Mesh of Quad4 Elements, ν = 1/3:

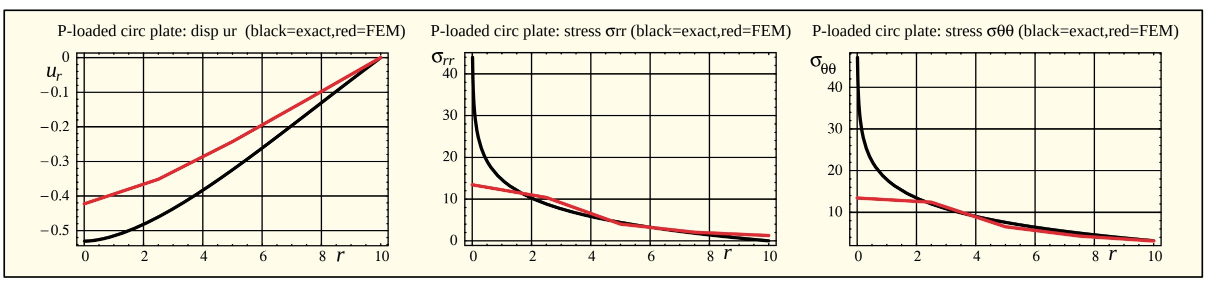

(b) 16 x 2 Mesh of Quad4 Elements, ν = 1/3:

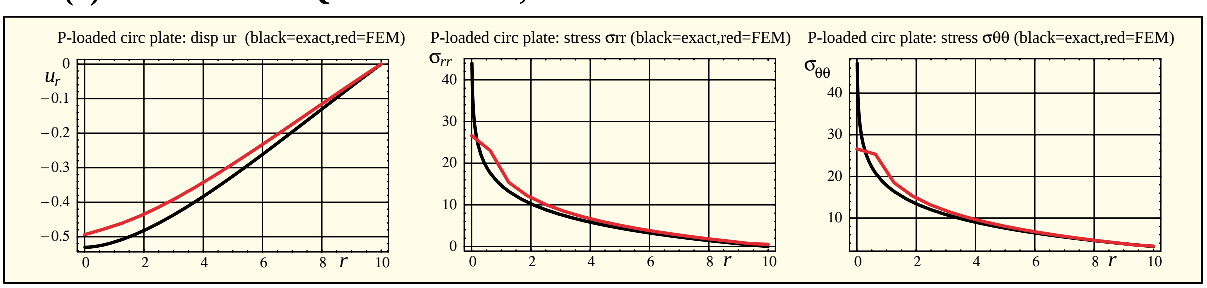

FIGURE 14.21. Point loaded circular plate benchmark: radial plots of u_r, σ_{rr} and $\sigma_{\theta\theta}$ for 4 × 2 and 16 × 2 element Quad4, with Poisson ratio $\nu = 1/3$. Plot is along the bottom plate surface $z = -h/2$.

Computed solution

node	r-disp	z-disp	sigma-rr	sigma-zz	sigma-θθ	sigma-rz	r-force	z-force
1	0.0000	-0.5381	17.7424	0.3592	17.7424	1.9099	-1.3263	-0.2653
2	0.0000	-0.5409	0.0000	0.0000	0.0000	1.9099	0.0000	-1.0610
3	0.0000	-0.5381	-17.7424	-0.3592	-17.7424	1.9099	1.3263	-0.2653
4	0.0223	-0.4676	10.2753	0.0000	12.3574	0.9549	0.0000	0.0000
5	-0.0223	-0.4676	-10.2753	0.0000	-12.3574	0.9549	0.0000	0.0000
6	0.0308	-0.3265	3.4321	-0.0939	7.1442	0.1469	0.0000	0.0000
7	0.0000	-0.3274	0.0000	0.0000	0.0000	0.1469	0.0000	0.0000
8	-0.0308	-0.3265	-3.4321	0.0939	-7.1442	0.1469	0.0000	0.0000
9	0.0330	-0.1641	1.9422	0.0626	5.1496	0.2204	0.0000	0.0000
10	-0.0330	-0.1641	-1.9422	-0.0626	-5.1496	0.2204	0.0000	0.0000
11	0.0318	0.0002	-0.1718	-0.0462	2.9832	0.1469	0.0000	0.0000
12	0.0000	0.0000	0.0000	0.0000	0.0000	0.1469	0.0000	1.5915
13	-0.0318	0.0002	0.1718	0.0462	-2.9832	0.1469	0.0000	0.0000

Thin plate (Kirchhoff) solution

node	r-disp	z-disp	sigma-rr	sigma-zz	sigma-θθ	sigma-rz
1	0.0000	-0.5305	43.9761	0.0000	47.1592	0.0000
2	0.0000	-0.5305	0.0000	0.0000	0.0000	0.0000
3	0.0000	-0.5305	-43.9761	0.0000	-47.1592	0.0000
4	0.0227	-0.4606	8.8254	0.0000	12.0085	0.0000
5	-0.0227	-0.4606	-8.8254	0.0000	-12.0085	0.0000
6	0.0306	-0.3243	4.4127	0.0000	7.5958	0.0000
7	0.0000	-0.3243	0.0000	0.0000	0.0000	0.0000
8	-0.0306	-0.3243	-4.4127	0.0000	-7.5958	0.0000
9	0.0330	-0.1634	1.8314	0.0000	5.0145	0.0000
10	-0.0330	-0.1634	-1.8314	0.0000	-5.0145	0.0000
11	0.0318	0.0000	0.0000	0.0000	3.1831	0.0000
12	0.0000	0.0000	0.0000	0.0000	0.0000	0.0000
13	-0.0318	0.0000	0.0000	0.0000	-3.1831	0.0000

FIGURE 14.22. Point loaded circular plate benchmark: computed results and exact solution for 2×1 `Quad8` mesh, with Poisson ratio $\nu = 1/3$.

(a) 2 x 1 Mesh of Quad8 Elements, ν = 1/3:

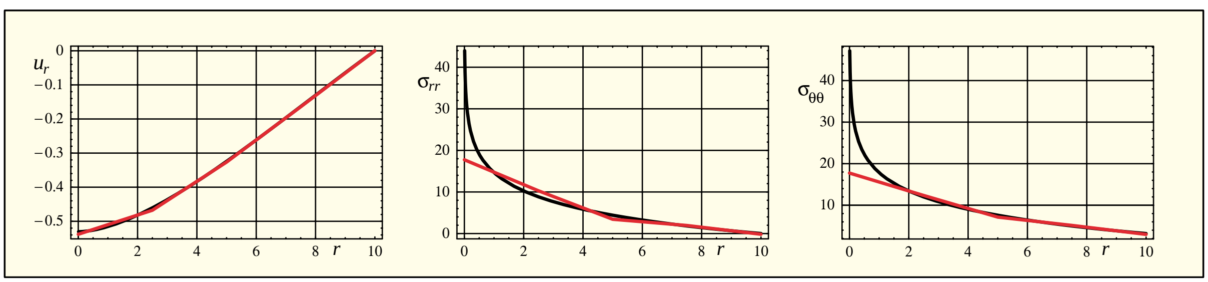

(b) 8 x 1 Mesh of Quad8 Elements, ν = 1/3:

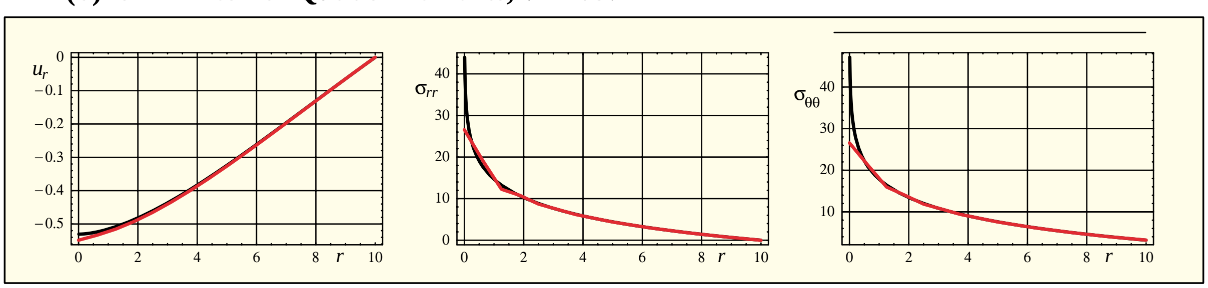

FIGURE 14.23. Point loaded circular plate benchmark: radial plots of u_r, σ_{rr} and $\sigma_{\theta\theta}$ for 2×1 and 8×1 `Quad8` meshes, with Poisson ratio $\nu = 1/3$. Plot is along the bottom plate surface $z = -h/2$.

Homework Exercises for Chapter 14
Axisymmetric Solid Benchmark Problems

EXERCISE 14.1 [C:20] This exercise deals with the thick-tube benchmark example discussed in §13.2–5. The script for this exercise is in Cell 12 of the Notebook `Quad4SOR.nb` supplied with this Chapter.

(a) Repeat the 4-element analysis using $\nu = 0.45$ and $\nu = 0.499$. Describe what happens to the accuracy of displacements and stresses when compared with the exact solution.

(b) Can a more refined mesh fix the problems noted in (a)? To check, run 16 elements along the radial direction and report if things have improved.

EXERCISE 14.2 [C:20] A concrete pile embedded in a soil half-space, as defined in Figure E14.1. This problem is solved using a very coarse mesh in Cell 17 of the Notebook `Quad4SOR.nb` supplied with this Chapter. Repeat the analysis using a more refined mesh, like that suggested in the figure. Module `GenerateGradedRingNodeCoordinates` may be used to generate a graded regular mesh.

The total force applied to pile is $P = 500000$ lbs (this may be assumed to be uniformly distributed on the top pile surface, or placed as a point load). Other data: pile modulus $E_P = 300,000$ psi, soil modulus $E_S = E_P/50$, Poisson's ratio for pile $\nu_P = 0.1$, Poisson's ratio for soil $\nu_S = 0.40$, pile diameter $d = 10$ in, pile length $L = 250$ in, and mesh z-length $H = 1.2L$. Truncate the mesh at $R = 80$ in. Neglect all body forces.

Nodes on the "soil truncation boundary" should be fixed. Points on the z axis $r = 0$ should be on vertical rollers except for 1.

The most interesting numerical results are: (i) the top and bottom vertical displacement of the pile, (ii) the reaction forces at the bottom of the pile, and (iii) the normal stress σ_{zz} in the pile.

EXERCISE 14.3 [C:20] The spinning Mother Earth. Model one quadrant of the planet cross section with an axisymmetric finite element mesh as sketched in Figure E19.3 (note that all elements are 4-node quadrilaterals). The problem is solved in Cell 18 of the Notebook `Quad4SOR.nb` supplied with this Chapter, using a very coarse mesh of only 4 elements.

Use the Kg-force/m/sec unit system for this problem. The Earth spins with angular velocity $\omega = 2\pi$ rad/24hrs $= (2\pi/86400)$ sec^{-1} about the z axis. The planet radius is $R = 6370$ Km = 6.37 10^6m. For E take 1/3 of the rigidity of steel, or E = 7 10^5 Kg/cm^2 = 7 10^9 Kg/m^2 as Love (Theory of Elasticity) recommends; Poisson's ratio $\nu = 0.3$ (this is my own guess), and mass density $\rho = 5.52$ times the water density. [Watch out for units: the centrifugal body force $\rho\omega^2 r$ should come up in Kg/m^3.] All gravitational field effects (self weight) are ignored.

(a) Get the equatorial "bulge" and the polar "flatening" in Km, and the maximum stress in MPa.

(b) Where do the maximum normal stresses occur?

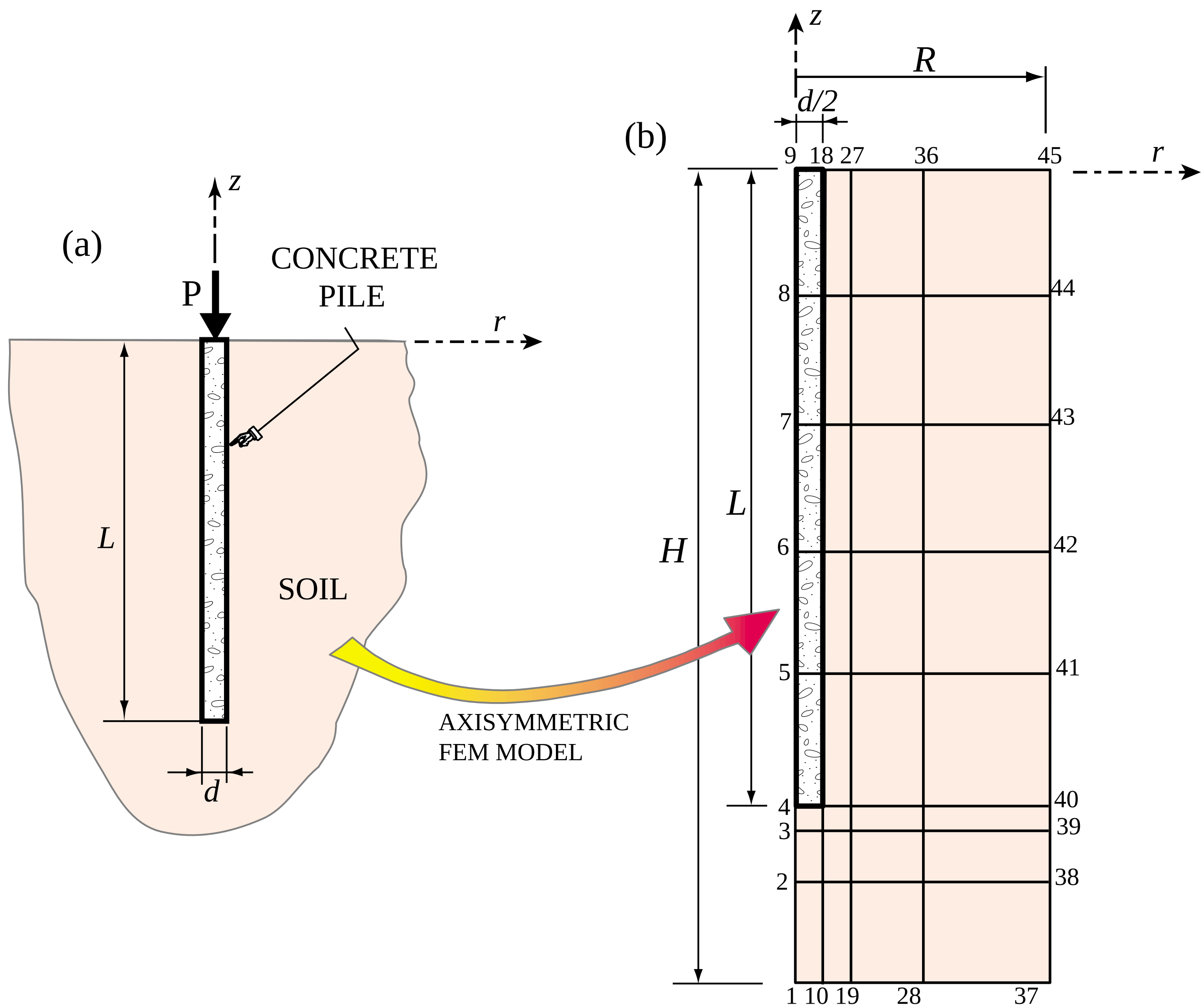

Figure E14.1. Pile embebded in soft soil.

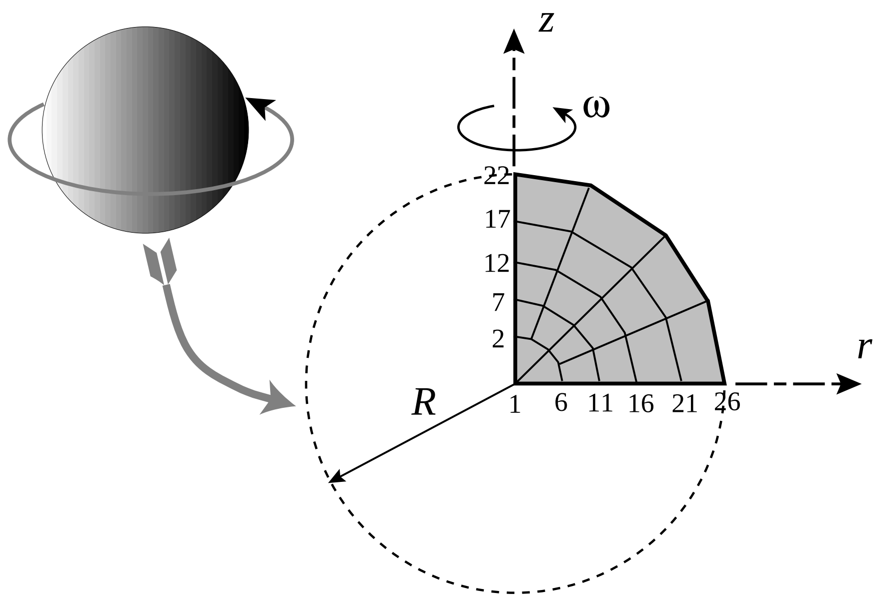

Figure E14.2. Our spinning planet.